Supplement of Atmos. Chem. Phys., 23, 5467–5486, 2023
https://doi.org/10.5194/acp-23-5467-2023-supplement

Atmospheric Chemistry and Physics
Open Access

Supplement of

Impact of solar geoengineering on wildfires in the 21st century in CESM2/WACCM6

Wenfu Tang et al.

Correspondence to: Wenfu Tang (wenfut@ucar.edu)

Extension for Section 3. Future trends of burned area and fire carbon emissions under the SSP scenarios

In terms of the spatial distribution, different regions exhibit diverse (even opposite) trends in both burned area and fire carbon emissions even in different ensemble members under the same SSP scenarios (Figures S3 and S4). And for a given region, different SSP scenarios can also lead to different trends. The 40°N–70°N latitude is the only latitude band in which the burned area consistently increases under all the SSP scenarios (Figure 1b). In the 0°–20°N and 30°S–10°S latitude bands, the trends in burned area varies substantially. In the 10°S–5°N latitude band (tropical region), the burned area consistently decreases under all seven scenarios to a diverse extent. The decreased burned area (possibly due to the reduced deforestation) in the tropical region is consistent with previous studies (e.g., Veira et al., 2016).

Even though fire carbon emissions are largely driven by burned area, they are also impacted by fuel availability and combustion completeness. Therefore, the fire carbon emissions and burned area generally show trends consistent with burned area, with some notable differences (Figures S3 and S5). As shown in Figures 1c and 1d, the projected trends in the fire carbon emissions are different from the trends in burned area in some cases, mainly due to the differences in the 2021-2030 period. A peak (Figure 1c) exists in the time series of fire carbon emissions between 2021-2030 under the SSP5-8.5 scenario. This is mainly due to the LULCC over Africa under SSP5-8.5 (i.e., there are peaks during 2020-2040 for both Northern Hemisphere Africa and Southern Hemisphere Africa under SSP5-8.5 and SSP5-8.5-based geoengineering scenarios, which however do not exist in the time series of burned area). The fire carbon emissions in the year 2015 under the SSP2-4.5 are significantly higher than the other scenarios, and decrease dramatically during 2015-2040, which is mainly driven by the change in South America (Figures S3 and S4). If considering the trends between 2040-2100, the trends of fire carbon emissions are overall consistent with the trends of burned area. I.e., the global total fire carbon emissions are projected to increase under the SSP scenarios (SSP1-2.6, SSP2-4.5, SSP3-7.0, and SSP5-8.5). In terms of the zonal change, the 40°N–70°N latitude band is still the only band in which the fire carbon emissions consistently increase under all SSP scenarios (Figure 1d). The differences in latitudinal changes between burned area and fire carbon emissions mainly exist in the 0°–20°N and 30°S–10°S latitude bands.

Regionally speaking, increases in both burned area and fire carbon emissions are projected under all the scenarios over Boreal North America, Temperate North America, Europe, Middle East, Boreal Asia, Central Asia, and Australia and New Zealand, when comparing 2091-2100 to 2021-2030 (Table S2). The strongest relative increase is seen over Boreal North America (Tables S2 and S3). Under the SSP5-8.5 and SSP3-7.0, the burned area and fire carbon emissions over Boreal North America are about three times higher in 2091-2100 compared to 2021-2030 – the relative change in burned area and fire carbon emissions are 314% and 345% under SSP5-8.5 and 306% and 288% under SSP3-7.0, respectively. In regions with consistently increasing trends, SSP-8.5 generally gives the strongest increase in burned area and fire carbon emissions, except for Temperate North America. Over Temperate North America, SSP3-7.0 leads to the strongest increase in 2091-2100 (~113%), followed by SSP5-8.5 (~50%). We note that over Central America,

burned area is consistently larger in 2091-2100 than in 2021-2030 under all scenarios, and fire carbon emissions are also consistently higher in 2091-2100 under most scenarios except for SSP2-4.5. Over Boreal Asia, burned area is larger under most scenarios (~22%–244%) in 2091-2100. As for fire carbon emissions, however, they are consistently higher in 2091-2100 under all scenarios (Table S2). In contrast, South America and Southeast Asia are projected to have less burned area and fire carbon emissions in 2091-2100 compared to 2021-2030 under all the SSP scenarios.

Table S1. Summary of WACCM6 simulations used in this study. Descriptions of scenarios can be found in Section 2.3.

Scenario	Number of simulations	Start year	End year
SSP1-2.6	1	2015	2100
SSP2-4.5	5	2015	2100
SSP3-7.0	1	2015	2100
SSP5-8.5	5	2015	2100
G6Sulfur	2	2015	2100
G6Solar	2	2015	2100

Table S2. Projected regional and global change of burned area and fire carbon emissions in 2091-2100 relative to 2021-2030 (%) under the SSP1-2.6, SSP2-4.5, SSP3-7.0, SSP5-8.5, G6solar, and G6sulfur. For the scenarios with multiple simulations, the ranges of the projection are also shown in the parentheses. The definition of the regions (Figure S3) follows Giglio et al. (2010), namely Boreal North America (BONA), Temperate North America (TENA), Central America (CEAM), Northern Hemisphere South America (NHSA), Southern Hemisphere South America (SHSA), Europe (EURO), Middle East (MIDE), Northern Hemisphere Africa (NHAF), Southern Hemisphere Africa (SHAF), Boreal Asia (BOAS), Central Asia (CEAS), Southeast Asia (SEAS), Equatorial Asia (EQAS), and Australia and New Zealand (AUST).

	Burned area change in 2091-2100 relative to 2021-2030 (%)					
	SSP1-2.6	SSP2-4.5	SSP3-7.0	SSP5-8.5	SSP5-8.5 G6solar	SSP5-8.5 G6sulfur
BONA	64.1	172	306	314	127	55.5
TENA	18.1	32.6	113	49.5	5.84	5.26
CEAM	2.13	8.72	34.6	92.4	47.8	49.6
NHSA	-37.8	-53.4	-37.3	-26.9	-70.7	-50.9
SHSA	-7.99	-14.3	-18.2	-21.4	-46.7	-50.4
EURO	39	57.1	116	96.6	34.8	52.7
MIDE	28.7	25.4	57.1	96.5	72.3	76.9
NHAF	16	-5.13	-7.57	2.15	10.4	6.19
SHAF	-9.79	-3.62	10.1	31.5	2.2	-19.7
BOAS	47.6	115	157	244	65.3	21.6

CEAS	44	47.3	66.3	124	54.4	33.5
SEAS	-22.9	-1.6	-50	-53.6	-56.5	-65.1
EQAS	50.8	-14.3	-3.28	-5.66	-0.497	10.5
AUST	12.7	6.82	17.3	6.09	5.97	6.66
Global	3.64	0.803	9.63	20.1	-2.31	-11.1

Fire carbon emissions change in 2091-2100 relative to 2021-2030 (%)

	SSP1-2.6	SSP2-4.5	SSP3-7.0	SSP5-8.5	SSP5-8.5 G6solar	SSP5-8.5 G6sulfur
BONA	45.3	206	288	345	155	49.6
TENA	48	78.9	210	132	66.7	65.1
CEAM	10.6	-39.5	33.7	117	57.7	84.5
NHSA	-29.2	-69	-26.9	-71.9	-87.8	-79.8
SHSA	-3.85	-39	7.77	-19.8	-39.9	-42.4
EURO	52.8	58	145	104	45	61.2
MIDE	40.4	46.1	108	150	129	129
NHAF	16.9	3.88	14	-30	-23.1	-28.9
SHAF	-10	-3.47	4.53	-31.2	-40.1	-51.1
BOAS	76.6	155	180	202	32.6	35.5
CEAS	33.3	56.2	64.6	127	58.6	37.7
SEAS	-58	-8.18	-64.4	-82.8	-83.9	-86.2
EQAS	44.2	5.81	47	27.2	61.2	50.7
AUST	16.1	15.4	35.2	21.3	35.6	42
Global	2.27	-11.8	23.7	-6	-24.6	-30.3

Table S3. Averages of regional and global annual projected burned area (Mha/year) and fire carbon emissions in 2091-2100 under the SSP1-2.6, SSP2-4.5, SSP3-7.0, SSP5-8.5, G6solar, and G6sulfur scenarios. For the scenarios with multiple simulations, the ranges of the projection are also provided in the brackets. The definition of the regions (Figure S3) follows Giglio et al. (2010), namely Boreal North America (BONA), Temperate North America (TENA), Central America (CEAM), Northern Hemisphere South America (NHSA), Southern Hemisphere South America (SHSA), Europe (EURO), Middle East (MIDE), Northern Hemisphere Africa (NHAF), Southern Hemisphere Africa (SHAF), Boreal Asia (BOAS), Central Asia (CEAS), Southeast Asia (SEAS), Equatorial Asia (EQAS), and Australia and New Zealand (AUST).

	SSP1-2.6	SSP2-4.5	SSP3-7.0	SSP5-8.5	SSP5-8.5 G6solar	SSP5-8.5 G6sulfur
			Burned area (Mha/year) 2091-2100			
BONA	2.57	3.14	5.47	6.27	3.11	2.11
TENA	9.83	11.6	18.8	12.6	9.15	9.03
CEAM	13.8	13.6	15.3	22	16	16
NHSA	3.05	3.5	3.39	5.91	2.48	3.76
SHSA	102	95.8	85.9	73.4	48.9	43.3
EURO	12.9	15.6	21	19.4	13.9	15
MIDE	8.79	8.74	10.4	14.2	12.6	12.7
NHAF	104	82.2	77.7	95.5	109	101
SHAF	117	123	134	180	140	118
BOAS	6.15	5.73	9.57	9.93	4.26	3.19
CEAS	48.5	47.4	56	70.8	48.6	43.5
SEAS	13.9	15.3	8.47	8.44	8.13	6.03
EQAS	1.03	1.47	0.973	0.811	0.701	0.681
AUST	44.9	47	56.7	49.8	49.9	43.6
Global	499	486	516	583	478	430
			Fire carbon emissions (Tg/year) 2091-2100			
BONA	55.1	77.8	120	154	72.5	48.5
TENA	45.7	59.5	101	74.8	55.8	54.8
CEAM	75.4	62.7	82.2	125	88.5	101
NHSA	40.7	59.4	46.2	58.9	26.7	42.2
SHSA	588	695	619	387	289	264
EURO	74.4	86.3	129	113	84.8	87.2
MIDE	43.7	46.7	59.7	80.7	75.7	74
NHAF	291	270	265	294	331	312
SHAF	441	467	486	617	526	466
BOAS	118	110	181	152	62.8	54.6
CEAS	249	272	308	395	275	242
SEAS	83.4	211	68.3	45.4	44	36.2
EQAS	40.7	58.6	56.4	39.3	36.6	36.6
AUST	132	145	189	164	180	169
Global	2.38×10^3	2.73×10^3	2.83×10^3	2.83×10^3	2.26×10^3	2.1×10^3

* 1 Mha equals to 10^4 km^2.

Table S4. 1-year lag correlations of precipitation change and burned area change and fire carbon emission change for SSP2-4.5, G6Solar, and G6Sulfur from SSP5-8.5.

	Burned area			Fire carbon emissions		
	SSP2-4.5	G6Solar	G6Sulfur	SSP2-4.5	G6Solar	G6Sulfur
BONA (Boreal North America)	-0.12	-0.09	-0.06	-0.20	-0.15	-0.10
TENA (Temperate North America)	0.04	/	-0.05	0.04	/	/
CEAM (Central America)	-0.21	-0.15	/	-0.28	-0.19	/
NHSA (Northern Hemisphere South America)	/	/	-0.18	/	-0.11	-0.29
SHSA (Southern Hemisphere South America)	-0.11	-0.31	-0.25	-0.08	-0.24	-0.21
EURO (Europe)	-0.11	-0.15	0.07	-0.06	-0.04	0.11
MIDE (Middle East)	-0.21	-0.11	0.06	-0.21	/	0.15
NHAF (Northern Hemisphere Africa)	-0.11	-0.07	-0.06	-0.05	-0.05	-0.05
SHAF (Southern Hemisphere Africa)	-0.26	-0.13	-0.20	-0.19	-0.03	-0.07
BOAS (Boreal Asia)	-0.06	-0.13	-0.06	-0.08	-0.18	-0.07
CEAS (Central Asia)	-0.10	/	0.05	-0.06	0.03	0.06
SEAS (Southeast Asia)	/	-0.07	/	/	-0.07	/
EQAS (Equatorial Asia)	0.14	/	0.11	0.17	/	0.17
AUST (Australia and New Zealand)	0.05	-0.07	-0.03	0.05	-0.06	/

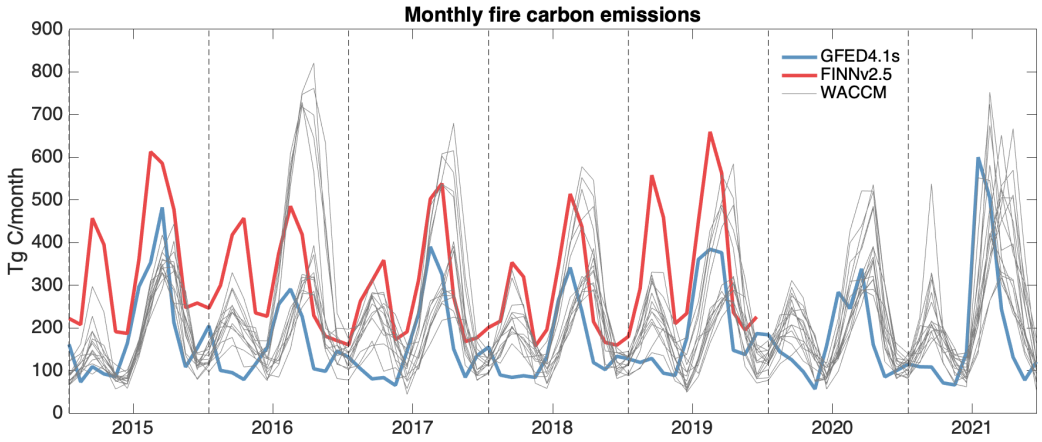

Figure S1. Monthly time series of global total fire carbon emissions from FINNv2.5, GFED4.1s, and WACCM simulations.

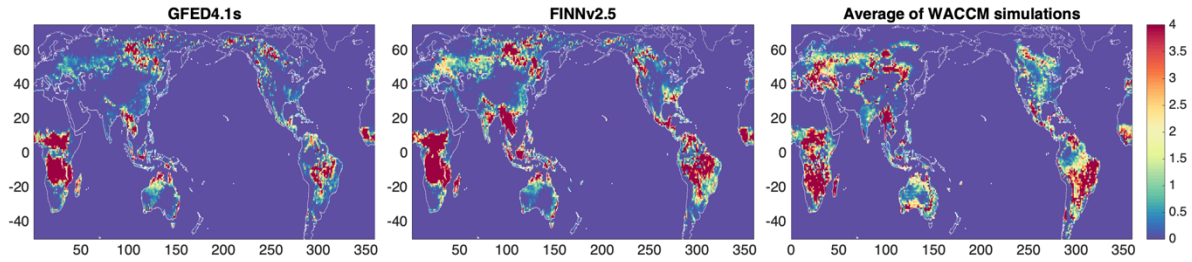

Figure S2. Spatial distribution of fire carbon emissions (gC/m^2/month) averaged from 2015 to 2019.

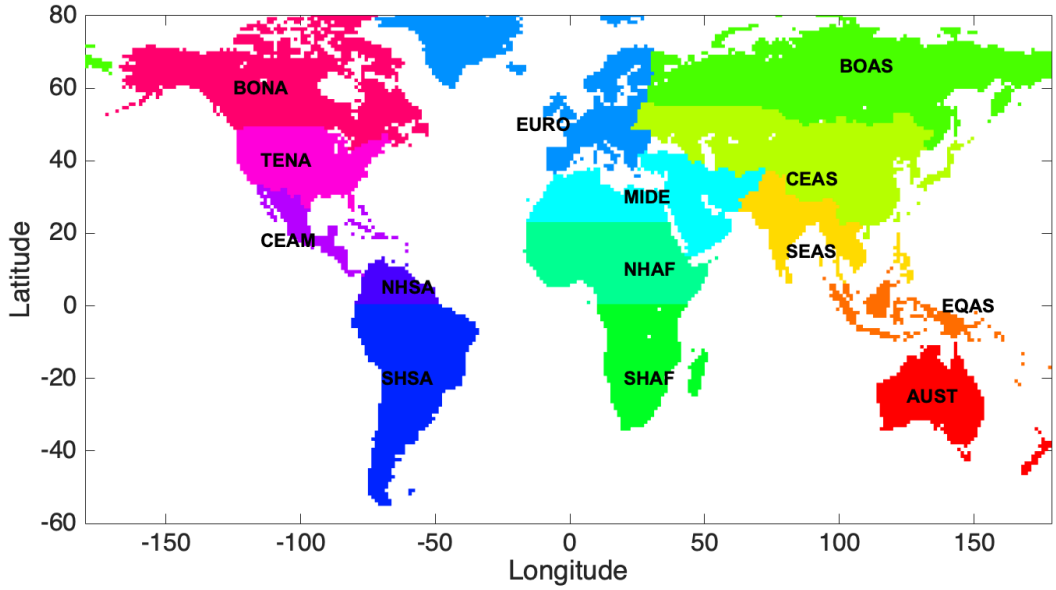

Figure S3. Region definition used in this study. The definition of the 14 regions follows Giglio et al. (2010), including BONA (Boreal North America), TENA (Temperate North America), CEAM (Central America), NHSA (Northern Hemisphere South America), SHSA (Southern Hemisphere South America), EURO (Europe), MIDE (Middle East), NHAF (Northern Hemisphere Africa), SHAF (Southern Hemisphere Africa), BOAS (Boreal Asia), CEAS (Central Asia), SEAS (Southeast Asia), EQAS (Equatorial Asia), and AUST (Australia and New Zealand).

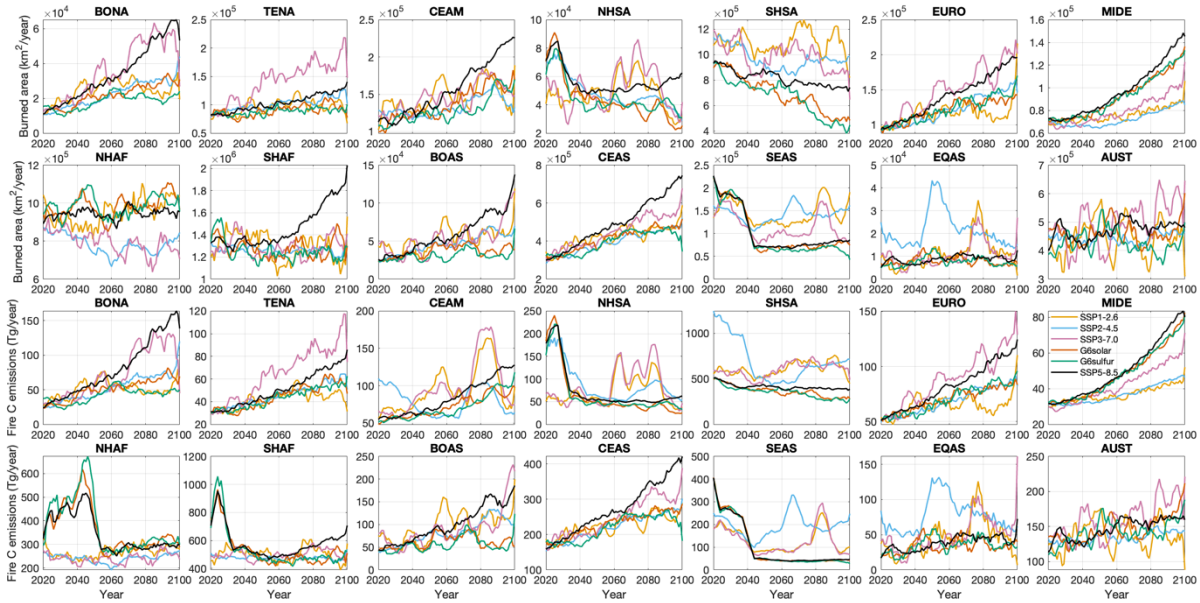

Figure S4. Time series of regional burned area (upper two rows) and fire carbon emissions (lower two rows) over BONA (Boreal North America), TENA (Temperate North America), CEAM (Central America), NHSA (Northern Hemisphere South America), SHSA (Southern Hemisphere South America), EURO (Europe), MIDE (Middle East), NHAF (Northern Hemisphere Africa), SHAF (Southern Hemisphere Africa), BOAS (Boreal Asia), CEAS (Central Asia), SEAS (Southeast Asia), EQAS (Equatorial Asia), and AUST (Australia and New Zealand). The time series are shown as 5-year moving average. The definition of the 14 regions follows Giglio et al. (2010). Simulations under the SSP1-2.6, SSP2-4.5, SSP3-7.0, SSP5-8.5, G6solar, and G6sulfur scenarios are represented by different colors.

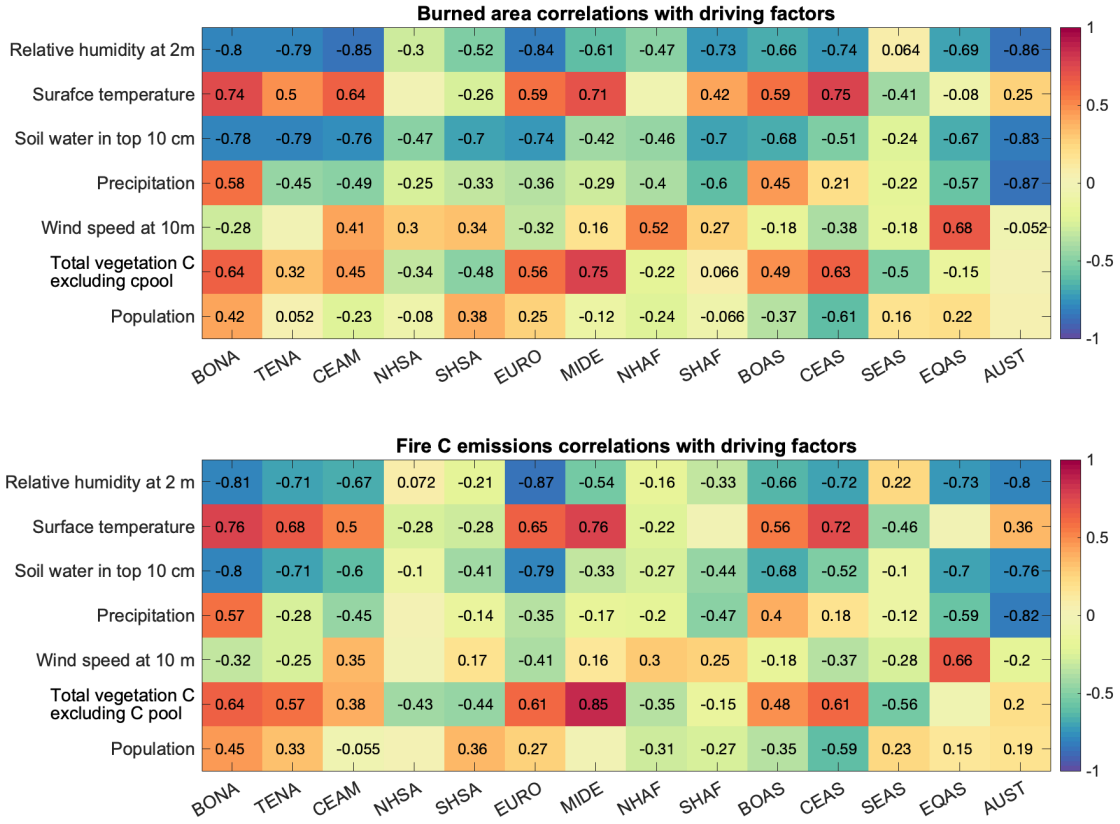

Figure S5. Correlations of burned area, fire carbon emissions with the driving factors (surface temperature, precipitation, relative humidity at 2 m, wind speed at 10 m, total vegetation carbon excluding carbon pool, and population) over 14 regions. The 14 regions are BONA (Boreal North America), TENA (Temperate North America), CEAM (Central America), NHSA (Northern Hemisphere South America), SHSA (Southern Hemisphere South America), EURO (Europe), MIDE (Middle East), NHAF (Northern Hemisphere Africa), SHAF (Southern Hemisphere Africa), BOAS (Boreal Asia), CEAS (Central Asia), SEAS (Southeast Asia), EQAS (Equatorial Asia), and AUST (Australia and New Zealand). The values of the correlations are labeled in the figure unless the correlation is not significant (P value > 0.1). The correlations are calculated based on the annual mean values of the variables, and all simulations are included in the calculation regardless of their scenarios.

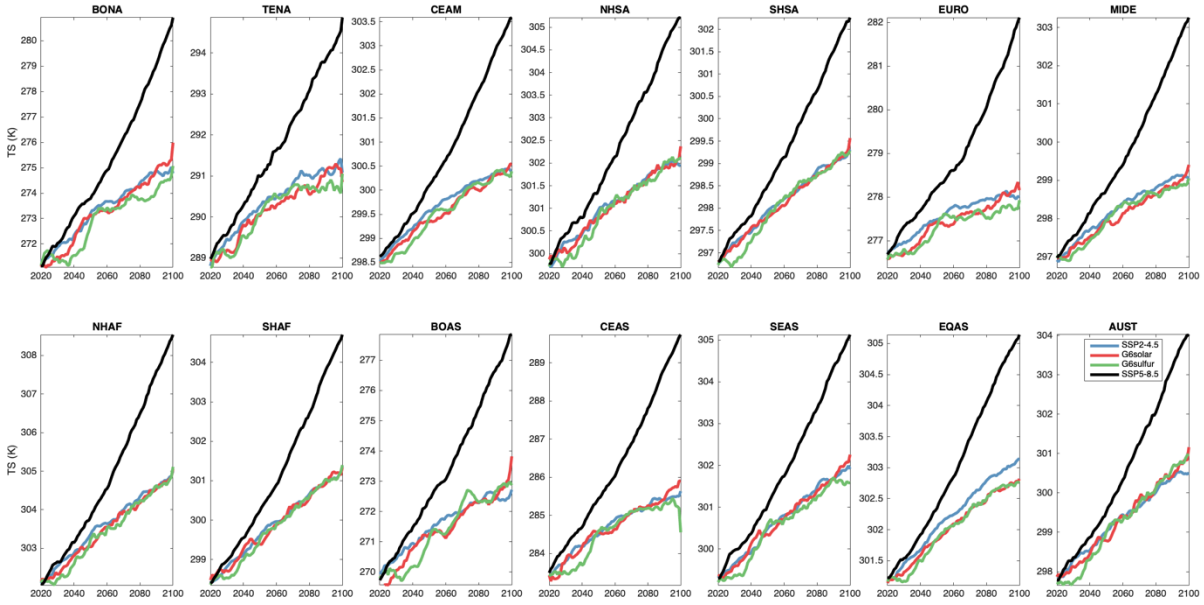

Figure S6. Time series of regional mean surface temperature under the SSP2-4.5, G6solar, G6sulfur, and SSP5-8.5 scenarios over BONA (Boreal North America), TENA (Temperate North America), CEAM (Central America), NHSA (Northern Hemisphere South America), SHSA (Southern Hemisphere South America), EURO (Europe), MIDE (Middle East), NHAF (Northern Hemisphere Africa), SHAF (Southern Hemisphere Africa), BOAS (Boreal Asia), CEAS (Central Asia), SEAS (Southeast Asia), EQAS (Equatorial Asia), and AUST (Australia and New Zealand). For the scenarios with multiple simulations, only simulation means are shown.

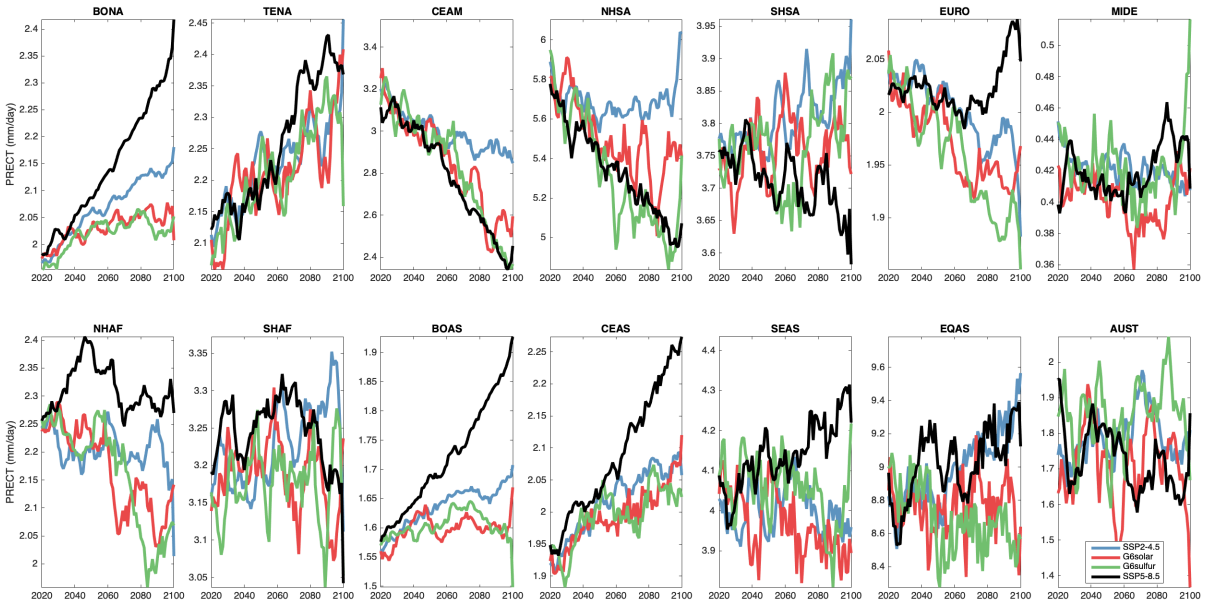

Figure S7. Same as Figure S6 but for precipitation (mm/day).

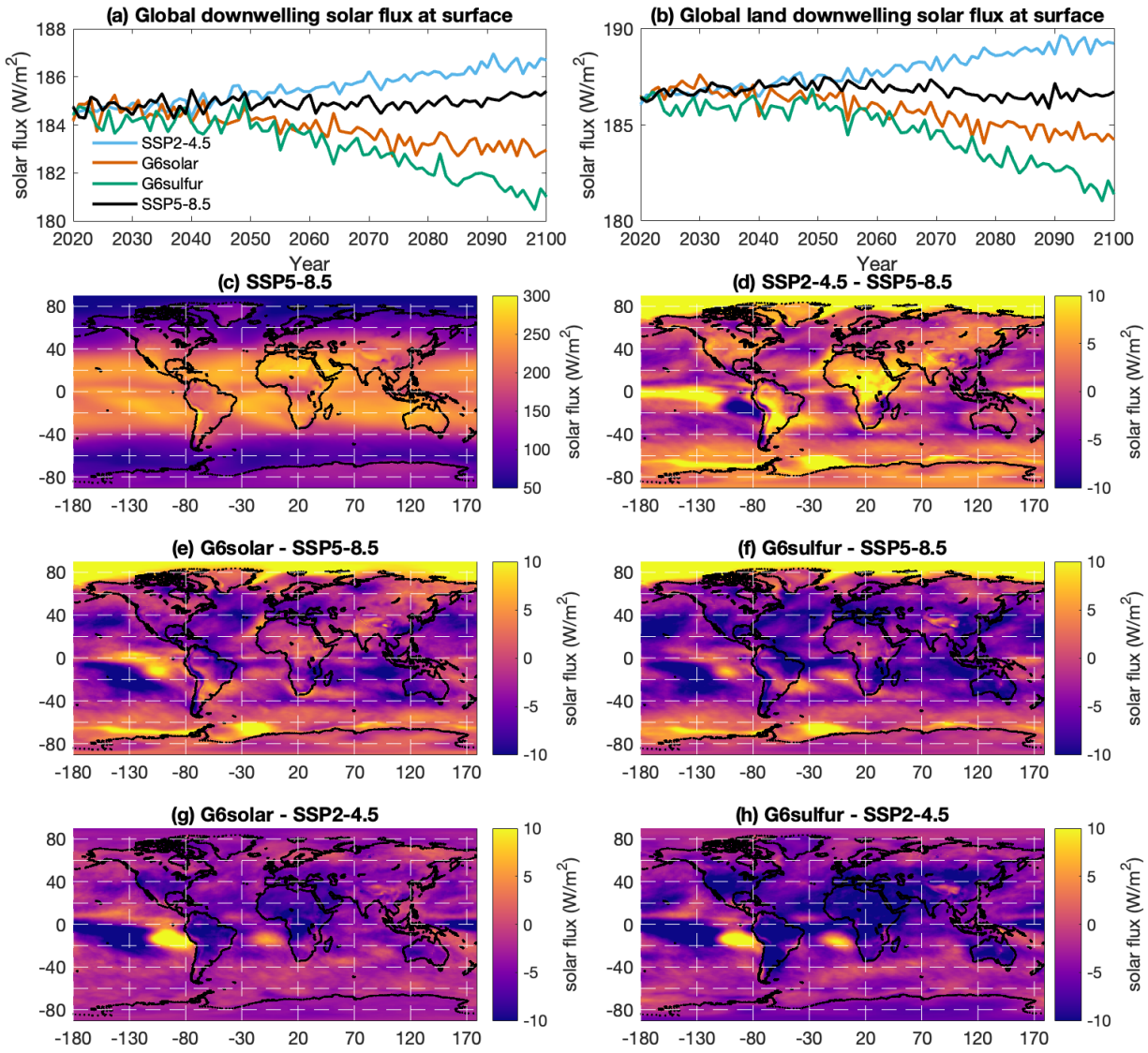

Figure S8. Time series of downwelling solar flux at surface (W/m^2) over (a) the whole global and (b) the land. (c) Spatial distribution of downwelling solar flux at surface (W/m^2) averaged for 2091-2100 under SSP5-8.5. The difference in downwelling solar flux at surface (W/m^2) of (d) SSP2-4.5 from SSP5-8.5 (e) G6Solar from SSP5-8.5, (f) G6Sulfur from SSP5-8.5, (g) G6Solar from SSP2-4.5, and (h) G6Sulfur from SSP2-4.5 averaged for 2091-2100. For a scenario with multiple simulations (i.e., SSP5-8.5, SSP2-4.5, G6Sulfur, and G6Solar), simulation means are shown.

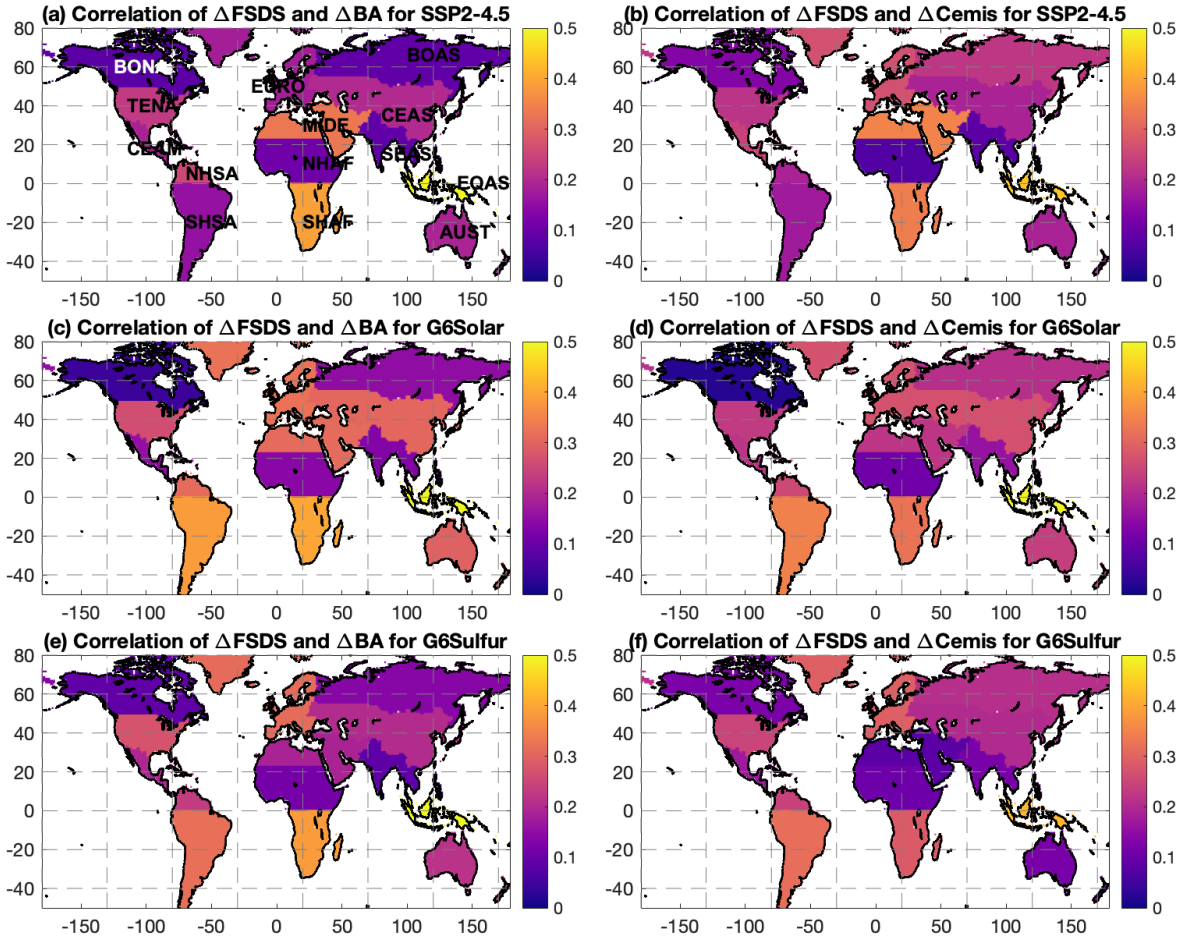

Figure S9. Correlations of (a) downwelling solar flux at surface change (ΔFSDS) and burned area change for SSP2-4.5, and (b) ΔFSDS and fire carbon emission change (ΔCemis) for SSP2-4.5. Only correlations that are significant are shown (p value <= 0.1). For SSP2-4.5, ΔTS is calculated for individual model grids within the region and annual values. It is defined as TS of SSP2-4.5 minus TS of SSP5-8.5 (the reference case). ΔBA and ΔCemis are defined in the same way as ΔTS. (c-d) are the same as (a-b) but for G6Solar; (e-f) are the same as (a-b) but for G6Sulfur. Correlations are calculated for 14 regions as labeled on the maps, following Giglio et al. (2010), namely Boreal North America (BONA), Temperate North America (TENA), Central America (CEAM), Northern Hemisphere South America (NHSA), Southern Hemisphere South America (SHSA), Europe (EURO), Middle East (MIDE), Northern Hemisphere Africa (NHAF), Southern Hemisphere Africa (SHAF), Boreal Asia (BOAS), Central Asia (CEAS), Southeast Asia (SEAS), Equatorial Asia (EQAS), and Australia and New Zealand (AUST). A corresponding table is provided in the supplement (Table S1).

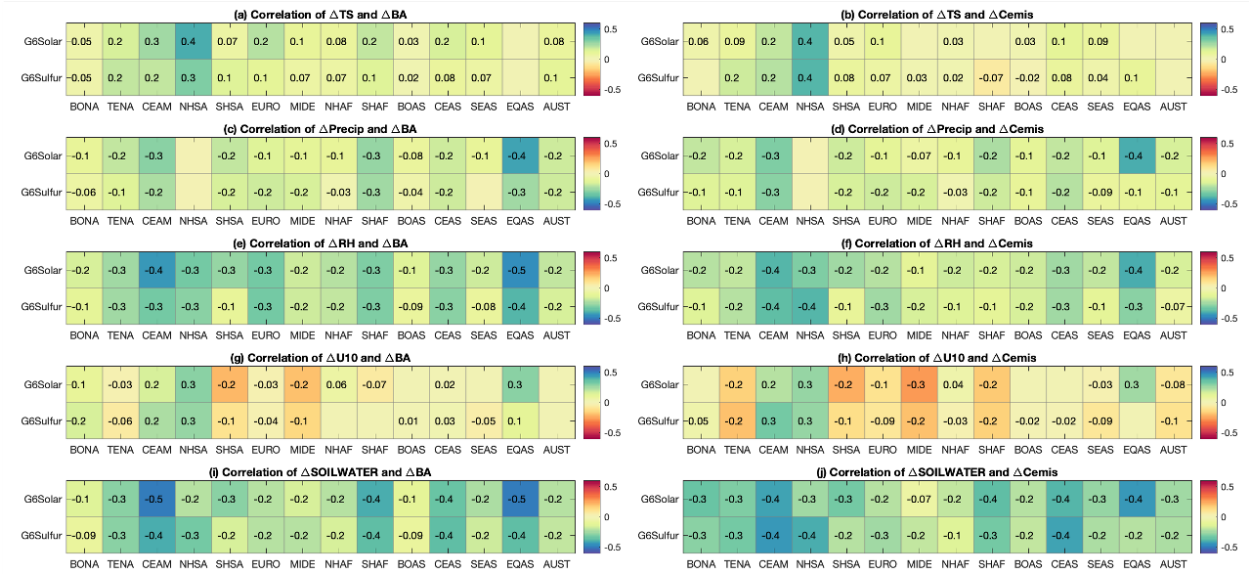

Figure S10. Same as Figure 6 but using SSP2-4.5 instead of SSP5-8.5 as the reference case.

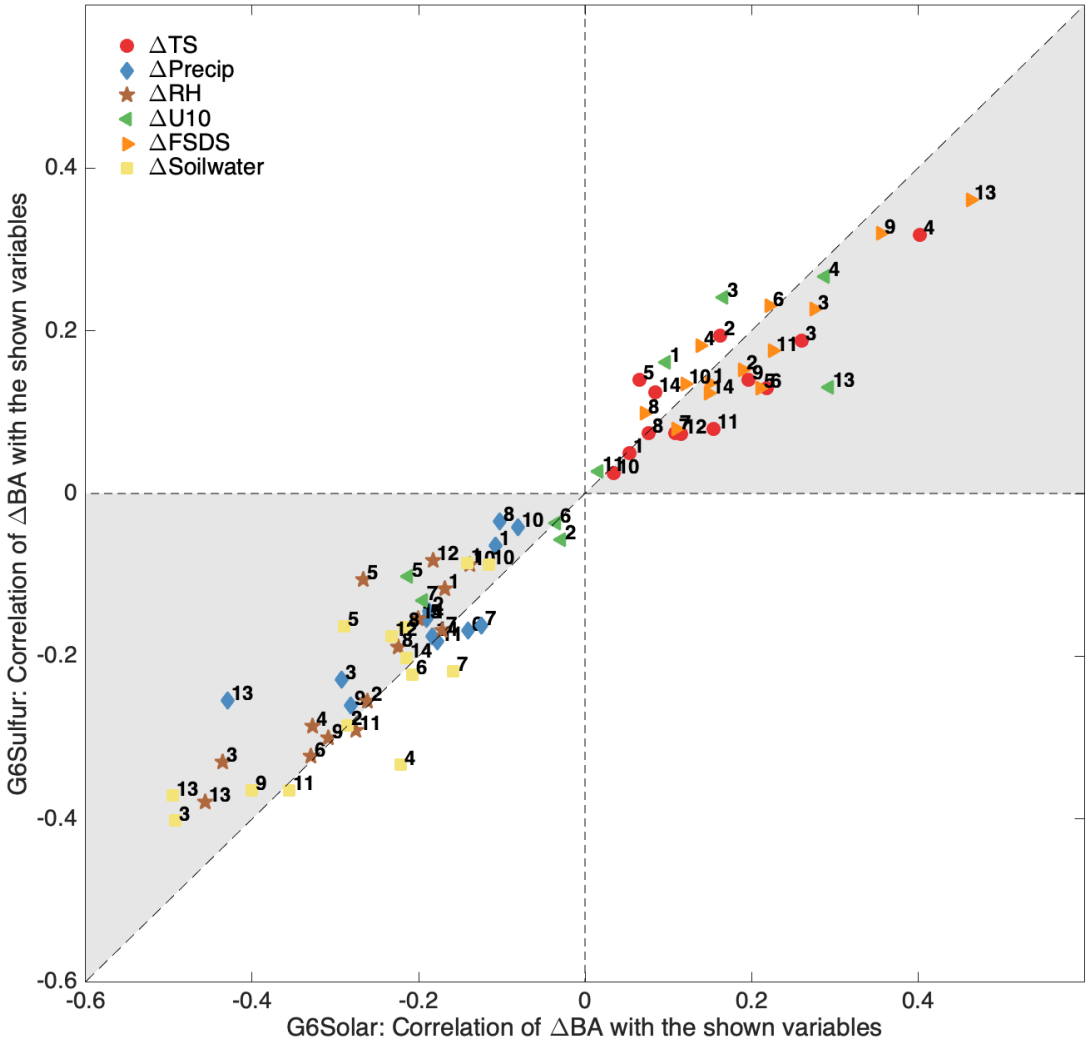

Figure S11. Same as Figure 15 but using SSP2-4.5 instead of SSP5-8.5 as reference case to calculate changes.

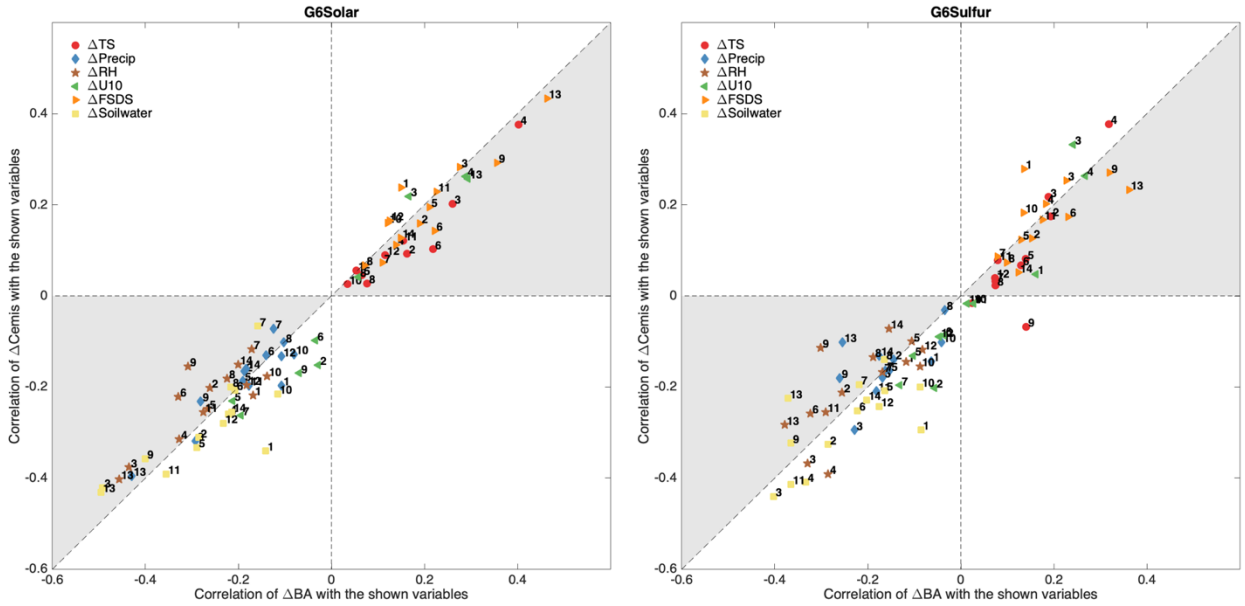

Figure S12. Same as Figure 16 but using SSP2-4.5 instead of SSP5-8.5 as reference case to calculate changes.

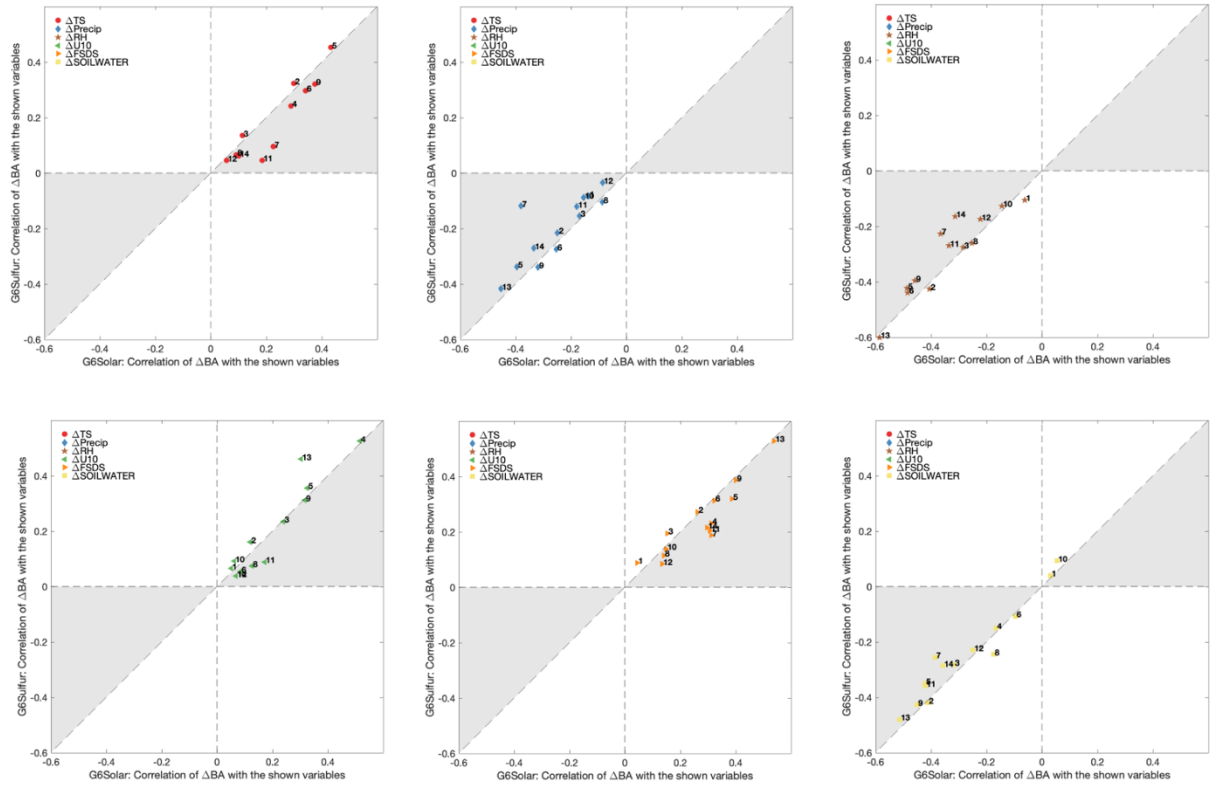

Figure S13. Same as Figure 8 but showing each variable separately.

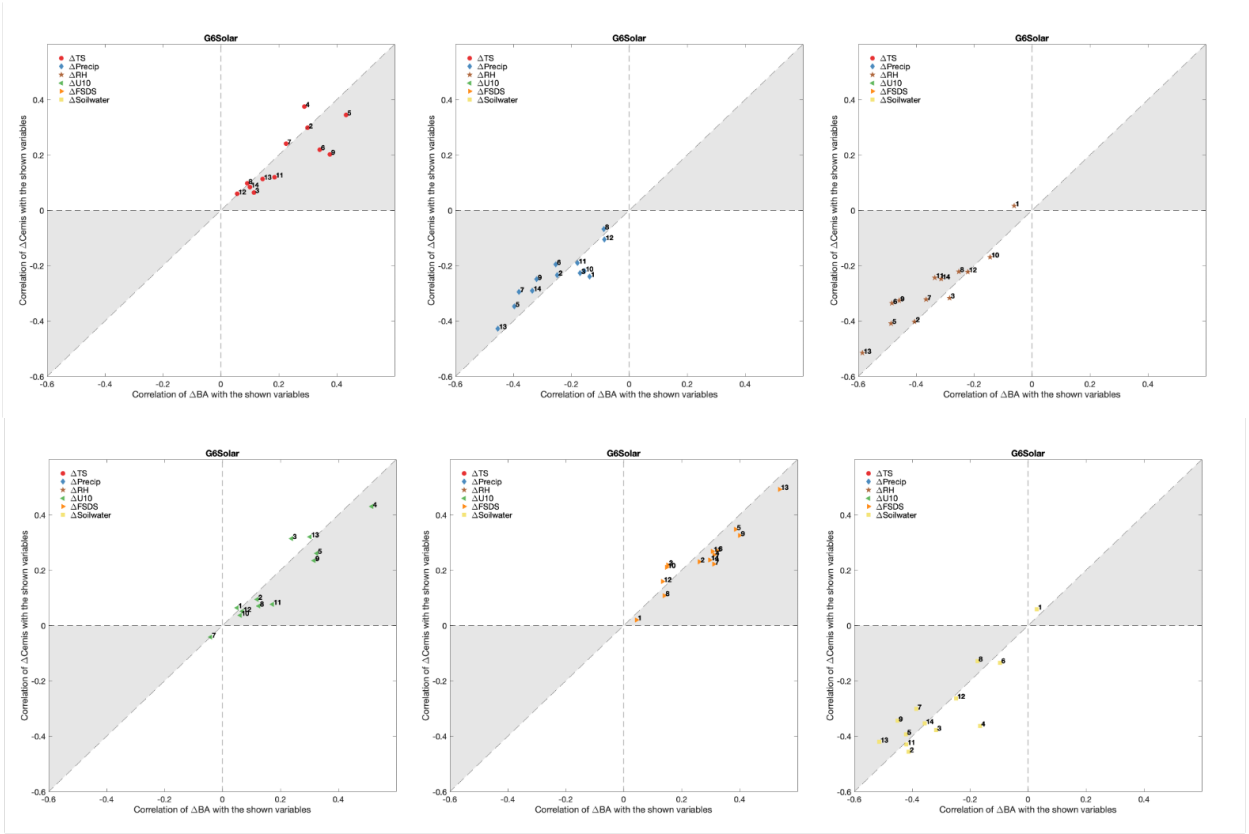

Figure S14. Same as Figure 9a but showing each variable separately.

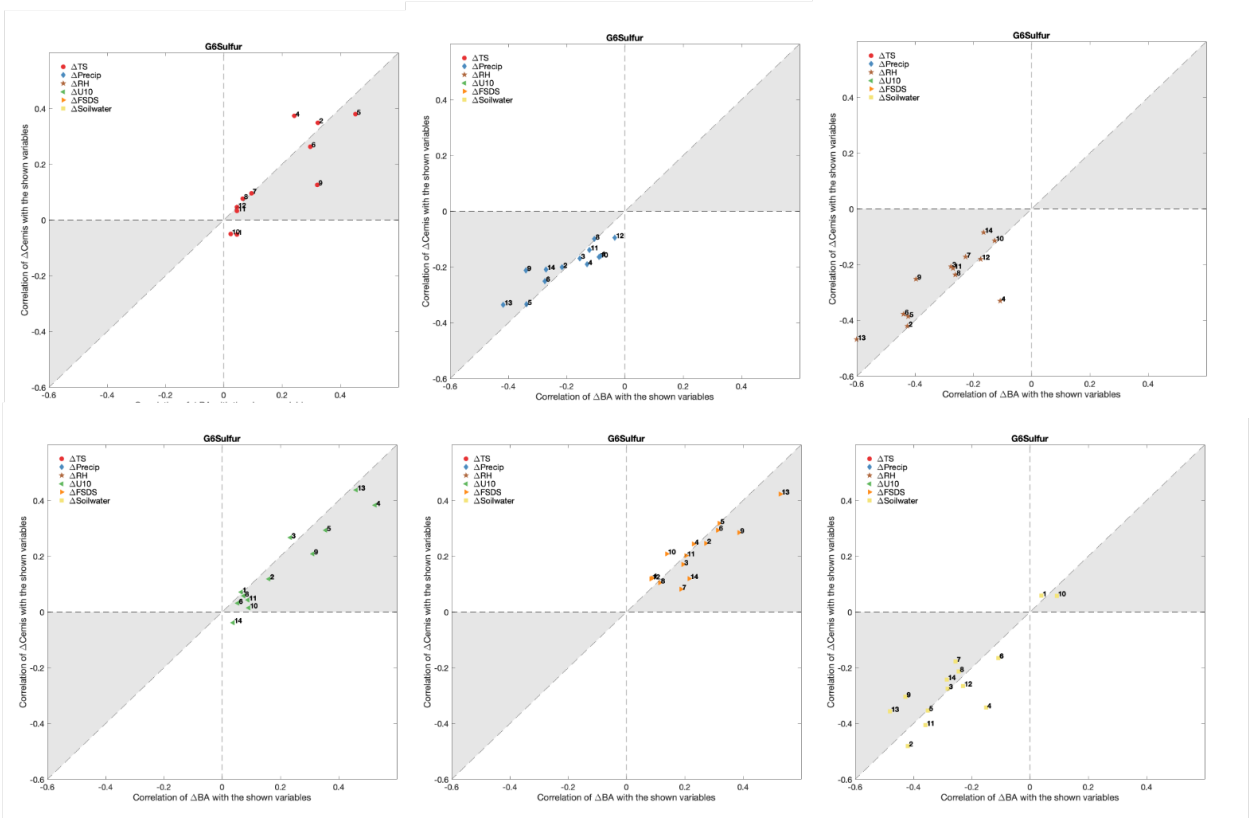

Figure S15. Same as Figure 9b but showing each variable separately.

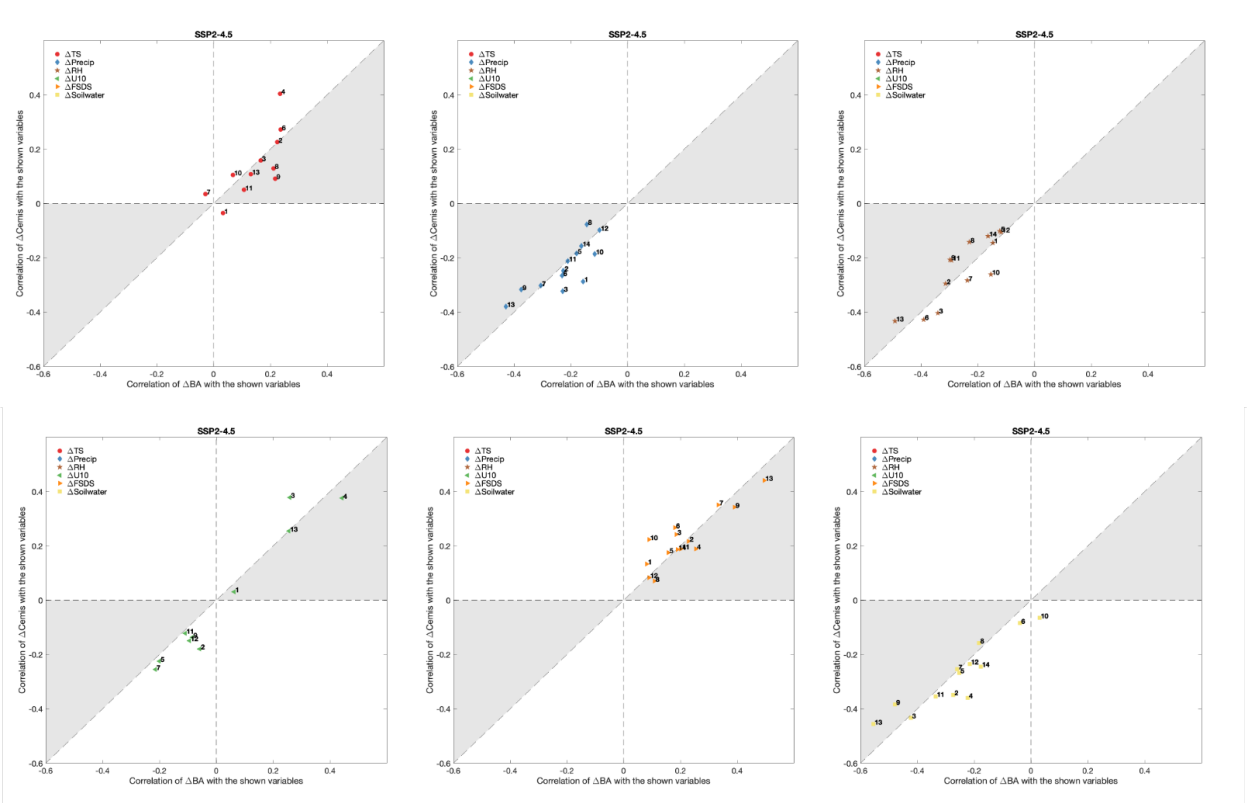

Figure S16. Same as Figure 9c but showing each variable separately.